A Comparison of Near-Surface Current Measurements by ADCP and HF-Radar on the West Florida Shelf

F. J. Kelly[1], J. S. Bonner[1], J. C. Perez[1], D. Trujillo[1], R. H. Weisberg[2], M. E. Luther[2] and R. He[2]
[1]Conrad Blucher Institute for Surveying and Science, Texas A&M University-Corpus Christi,
6300 Ocean Drive, Corpus Christi, TX, 78412, (361) 825-5520
[2]College of Marine Science, University of South Florida, 140 7th Avenue South, St. Petersburg, FL, 33701, (727) 553-1568
(fkelly@cbi.tamucc.edu), (bonner@cbi.tamucc.edu), (perez@cbi.tamucc.edu), (trujillo@cbi.tamucc.edu),
(weisberg@marine.usf.edu), (luther@marine.usf.edu), (ruoying@marine.usf.edu)

Abstract—Surface currents (0.5 m) were measured during an eleven-day deployment of a pair of CODAR Ocean Sensors 25-MHz SeaSonde™ HF-Radars. The radar footprint overlooked of an array of acoustic Doppler current profilers on the West Florida Shelf (WSF) located between the 10 m to 30 m isobaths. An earlier study compared the hourly-averaged HF-Radar current vectors at grid points near the ADCP moorings, and found correlation coefficients (R) of 0.8 to 0.9 for the alongshelf components but 0.6 or less for the cross-shelf components, which are small in magnitude. The study noted that the alongshelf surface currents measured by the radar are about 30% larger than those of the ADCPs measured 2 to 3 m below the surface according to standard deviations and linear regression slopes. In this study we focus on the mooring located near the center of the radar coverage and explore the near surface shear and wind forcing. A fit of the M_2 tide, which is barotropic on the WSF, to the ADCP and radar vector time series yielded current tidal ellipse parameters that are in close agreement, suggesting that the low-frequency, upper-layer shear may be real. Alongshelf wind and radar current speed (at 0.5 m) were more strongly correlated than the alongshelf wind and ADCP current at 2.5 m depth. Both the principal axis analyses and the complex vector correlations indicate directional differences of 6º to 12º counter-clockwise rotation (looking down) for currents with respect to wind, i.e., to the left of the wind, which is attributed primarily to the location of the coastal wind station.

I. INTRODUCTION

Over the past thirty years High-Frequency (HF) Radar has become a useful oceanographic tool for mapping the surface current layer and providing useful supplements to conventional oceanographic data [1]. In order to provide perspective on what HF Radar measures, studies have compared its observations with those from more conventional instruments, particularly the Acoustic Doppler Current Profiler (ADCP) (e.g., [2], [3], [4]). The general contrasting characteristics of the two instruments are that the radar yields a spatially and temporally averaged surface current measurement while the ADCP produces a subsurface point measurement. Nevertheless, comparison studies have reported good agreement, with the HF-Radar currents typically being stronger than those measured by the nearest-to-the-surface good ADCP bin.

The Conrad Blucher Institute for Surveying and Science (CBI) at Texas A&M University-Corpus Christi and the Texas Engineering Experiment Station (TEES) acquired a pair of SeaSonde® 25-MHz HF-Radar systems from CODAR Ocean Sensors for use in oil-spill response research and configured them in small trailers for mobile operation. CBI conducted an eleven-day deployment exercise in January 2001 in collaboration with the College of Marine Science at the University of South Florida (USF), which was operating six ADCP current-meter sites on the West Florida Shelf (WFS) south of Tampa Bay (Fig. 1). The radar's footprint had a maximum range of 60 km offshore and covered the mooring locations between the 10-m to 30-m isobaths. An earlier study [2] used a variety of metrics to analyze the correlation between the surface currents measured by the HF-Radar and the subsurface currents measured by the ADCPs. Scalar regression analysis found correlation coefficients (R) of 0.8 to 0.9 for the alongshelf components but 0.6 or less for the cross-shelf components. That study determined that, according to standard deviations and linear regression slopes, alongshelf surface currents measured by the radar are on the order of 30% larger than those of the ADCPs measured 2 m to 3 m below the surface.

As one test of the validity of the observed upper layer shear, we take advantage of the nature of the main tidal constituent on the WFS, the M_2 tide, which is low in amplitude but very barotropic [5]. We also examine the relative responses of the observed currents to local wind forcing.

II. METHODS

CBI deployed its mobile trailers containing the HF-Radars on the beaches at Anna Maria Key (HFR1) and Siesta Key (HFR2) as shown in Fig. 1, yielding a baseline distance of

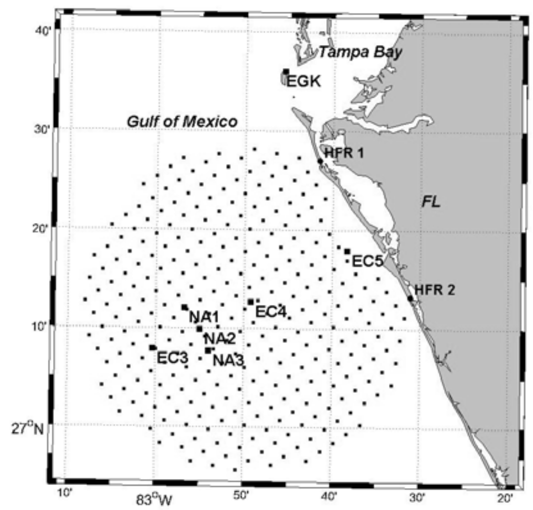

Fig. 1. Map showing coverage grid of the HF Radar, the two Radar sites (HFR1 and HFR2), the location of Egmont Key wind (EGK), and the USF ADCP mooring locations, including EC4 used in this study.

19.7 km. Table I provides details of the setup parameters for both sites. For this deployment, the actual antenna patterns were not measured, and bearing determination relied on ideal antenna patterns. However, the antennas at both sites were located on broad flat beaches with no near-field obstacles.

The HF-Radar system produced a total of 269 hourly surface current maps from 1600 UTC January 20 through 2000 UTC January 31, 2001 on a 3 km x 3 km grid. The 312 grid points shown in Fig. 1 correspond to those for which the angle of intersection of the radials from the two sites is greater than 30° and less than 150°. In this study we focus on the grid point (called HFR hereafter) that was closest to the ADCP mooring labeled EC4 in Fig. 1. HFR had 243 usable observations, while the EC4 data were continuous over the 269-hour period. The maximum range the radar is limited by the blanking time. Initially, this parameter was set to 243.2 μs or 36.5 km, which is just short of the USF moorings NA1, NA2 and NA3. At 0025 UTC January 26, 2001, about midway through the experiment, the blanking time was doubled, yielding a maximum range of 73 km.

TABLE 1
SEASONDE HF-RADAR CONFIGURATION PARAMETERS AND SPECIFICATIONS

SITE PARAMETERS		
	HFR1	HFR2
Latitude	27.2207° N	27.4498° N
Longitude	82.5182° W	82.6927° W
Operating Frequency	26.180 MHz	25.250 MHz
Water Wave Length	5.73 m	5.94 m
SEASONDE PARAMETERS		
Baseline Separation of Sites	19.7 km	
Number of Valid Measurement Cells	312	
Range Cell Resolution	3 km	
Measurement Cycle	60 minutes	
Angular Resolution	5°	
Map Vector Current Accuracy	< 7 cm s^{-1}	
Map Vector Direction Accuracy	< 10°	
Measurement Depth	0.5 m @ 26 MHz	

Table II presents the mooring and ADCP configuration for EC4. In this comparison study, we use only the topmost useable ADCP bin of data (2.5-m depth).

The ten-minute wind data recorded at Egmont Key (EGK in Fig. 1) were filtered with an eleven-point boxcar filter and sub-sampled to hourly values.

III. RESULTS

Vector time-series plots of the EGK wind, currents measured at the closest radar grid point to EC4 and the EC4 currents are shown in Fig. 2, which illustrates the characteristics of the two types of instruments noted earlier—radar currents are "smoother" that those from the ADCP because of the greater spatial and temporal averaging, and for this shallow near-shore location, the radar-measured surface currents (top 0.5 m) are somewhat stronger than those from the top ADCP bin located 2.5 m below the surface. The time-series plots also show the reversal in along-shelf flow that began about January 28th.

Winds recorded at EGK during the study were consistent with climatologic data for the region [6] [7]. During the first seven days (January 20-26) strong northwesterly (up to 12 m/s) and weaker northeasterly winds prevailed. A three-day transition period of weak and variable winds was followed by a switch to persistent southeasterly and southerly winds of about 5 m/s beginning on January 29th. HF-Radar surface current maps before and after the wind shift are shown in Fig.3. As might be expected, the coastal current patterns correspond to the direction an magnitude of wind forcing, with near shore waters responding more quickly to shifts in wind direction.

TABLE II
CONFIGURATION PARAMETERS FOR ADCP AT EC4

Site	EC4
Workhorse Model	300-kHz BB
Water Depth	20m
Top Bin Depth	2.5m
Bin size	0.5m
Orientation	Up
Mooring type	Bottom-mount
Latitude	27.2112
Longitude	-82.8206

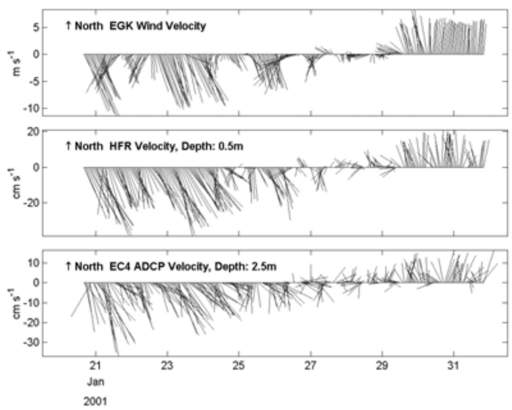

Fig. 2. Time-series stick vector plots of (top) EGK wind, (bottom) EC4 currents and (middle) the HF-Radar currents at the gridpoint closest to EC4.

Since the M_2 tide is barotropic on the WFS [5], we first performed a simple least-squares analysis for the 12.42-hour tidal period on the common 11.2-day records of HFR and EC4 currents and then calculated the tidal ellipse parameters (Table III). Although the length of the two time series is shorter than the 13-day minimum length required for standard harmonic analysis [8], we would expect the results to have similar magnitudes absent significant errors or bias in the HFR observations. The results support this expectation, with semi-major axes of 5.2 cm/s and 4.5 cm/s for the HFR and EC4 currents, respectively. Perhaps fortuitously, these values are close to the yearlong depth-averaged value of 4.5 cm/s for the EC4 mooring obtained by [5].

Currents in near-coastal regions are strongly steered by the topography, and the angle of the principal axis tends to parallel the coast. Therefore, time series of coastal currents are normally discussed in terms of a rotated coordinate system that has components parallel and perpendicular to the local topography. In this study we performed a principal component analysis on each current velocity time series and rotate it to the directions of the major and minor axes of its variance ellipse to obtain the most linearly independent orthogonal components [9], using the common 243 good points in each case. The results are shown in Table IV, which includes the angle from north of the major axis, and the magnitude of the major and minor axes in variance units (cm^2/s^2). In all subsequent analyses and discussion the term along-shelf refers to the component parallel to the major axis of a specific current vector time series. For the wind velocity we used an average of the principal axis values of the HFR and EC4 velocity series, because the wind is not couple to the bottom topography—but note that the angle of the principal axis of the wind velocity is only about ten degrees clockwise from that of the currents.

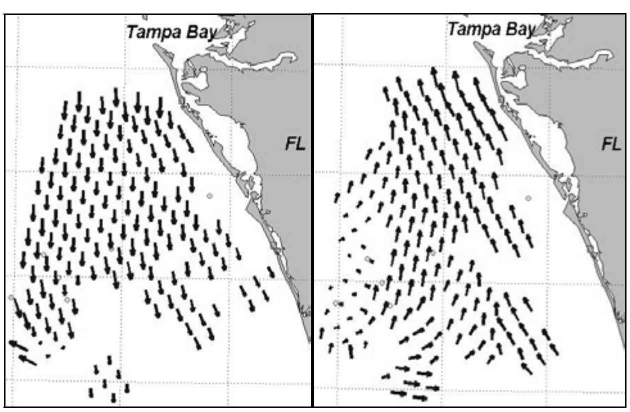

Fig. 3. Surface (0.5 m) current maps for 1/26/01 0600 UTC and 1/31/01 0500 UTC, showing current reversal after frontal passage.

TABLE II
CONFIGURATION PARAMETERS FOR ADCP AT EC4

Site	EC4
Workhorse Model	300-kHz BB
Water Depth	20m
Top Bin Depth	2.5m
Bin size	0.5m
Orientation	Up
Mooring type	Bottom-mount
Latitude	27.2112
Longitude	-82.8206

TABLE III
RESULTS OF ANALYSIS OF COMMON 243 POINTS FOR M_2 TIDAL COMPONENT, WHICH IS BAROTROPIC ON THE WFS, TOGETER WITH YEAR-LONG DEPTH AVERAGE OBTAINED BY REF. [5] FOR MOORING EC4.

SERIES	NUMBER OF POINTS	M2 TIDAL ELLIPSE	
		U-major (cm s^{-1})	U-minor (cm s^{-1})
EC4	243	5.2	-3.3
HFR	243	4.5	-2.3
EC4 (Ref [5])	Year-Long Depth Avg.	4.4	-2.7

TABLE IV
RESULTS OF THE PRINCIPLE AXIS ANALYSIS OF EACH VECTOR TIME SERIES: ANGLE OF MAXIMUM VARIANCE RELATIVE TO TRUE NORTH, MAJOR AND MINOR AXES (VARIANCE) OF PRINCIPLE ELLIPSE.

Current Meter	**Angle (°True)**	**Major Axis**	**Minor Axis**
		(cm^2/s^2)	**(cm^2/s^2)**
HFR	157.5	17.1	5.2
EC4	155.4	11.8	6.1
		(m^2/s^2)	**(m^2/s^2)**
EGK	165.9	5.1	2.1

Following the rotation of each vector series to the axes of its variance ellipse, we used linear regression and basic statistics to compare the alongshelf and cross-shelf components rather than spectral time-series analysis methods because of the short record lengths and data gaps. The "standard," linear, least-squares fitting assumes the abscissa values are error free and well known, which is not true for these data. There are uncertainties in the data of both series that we assume to have approximately equal weights, and we used the more general regression algorithm that allows for some uncertainties in both co-ordinates [10] [11] [12]. When the errors in both co-ordinates are equally weighted, the best-fit line is that which minimizes the sum of the squares of the perpendicular distance of the points from the line. A representative scatter plot and its regression line are shown in Fig. 4 for the alongshelf components of the EGK wind and HFR current time series shown in Fig. 2. Results of all regressions are summarized in Table V, and the basic statistics for each time series component are shown in Table VI. Following the method of Kundu [13], we also estimated the degree of correlation, γ, and the veering, θ, between the vector time series (Table VII).

The radar-derived surface current (0.5 m) shows stronger along-shelf flow in the mean, range and standard deviation than that of the ADCP-observations at 2.5 m depth. The standard deviation for the radar time series is larger than that for the ADCP by 5.4 cm/s (45%), and the slope from the linear regression analysis of the alongshelf components is 0.69, i.e., radar values are about 31% larger on average (Tables V and VI). Together, these metrics indicate that the alongshelf surface currents measured by the radar are significantly stronger than those of the ADCP. Cross-shelf statistics yield near-zero means and standard deviations that are small, i.e., on the order of 3 and 6 cm/s, respectively, which is comparable in magnitude to amplitude of the major axis of the M_2 tide (Table III). The work of [5] found that the M_2 tidal current ellipse at the EC4 mooring is oriented primarily in a cross-shelf direction.

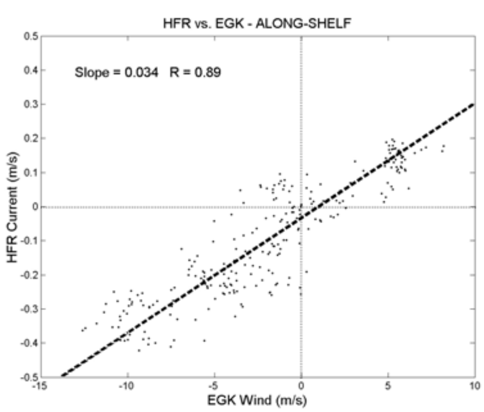

Fig. 4. Scatter plot and linear regression of alongshelf HF-Radar current speed (m/s) vs. EGK wind speed (m/s). Slope = 0.034, correlation coefficient R = 0.89.

TABLE V

REGRESSION RESULTS: SLOPE, INTERCEPT AND CORRELATION COEFFICIENT FOR GIVEN PAIR.

Regression Pair (Y vs. X)	Slope	Intercept (cm/s)	Correlation Coefficient (R)
Alongshelf			
HFR vs. EGK wind	0.034	-3.3	0.90
EC4 vs. EGK wind	0.023	-2.4	0.81
EC4 vs. HFR	0.69	-0.1	0.92
Cross Shelf			
HFR vs. EGK wind	0.023	-2.2	0.43
EC4 vs. EGK wind	0.027	-3.5	0.12
EC4 vs. HFR	1.16	-1.0	0.62

TABLE VI

BASIC STATISTICS, USING THE COMMON 243 POINTS, FOR EACH SERIES COMPONENT: MEAN, MINIMUM, MAXIMUM AND STANDARD DEVATION (CM/S). POSITIVE VALUES ARE UPCOAST AND OFFSHORE.

Series	Mean	Min.	Max.	Std.
Alongshelf				
EGK Wind (m/s)	-1.9	-12.5	8.4	5.1
HFR cm/s (cm/s)	-9.8	-42.1	19.7	17.1
EC4 cm/s (cm/s)	-6.9	-36.6	14.0	11.8
Cross Shelf				
EGK Wind (m/s)	0.6	-3.9	7.1	2.3
HFR cm/s (cm/s)	-0.8	-12.0	13.1	5.2
EC4 cm/s (cm/s)	-1.9	-14.6	16.4	6.1

TABLE VII

COMPLEX CORRELATION COEFFICIENTS, γ, AND THE ROTATION ANGLE, θ, FOR PAIRS OF THE EGK WIND, AND HF-RADAR, EC4 CURRENT VELOCITIES. POSITIVE θ INDICATES THE FIRST SERIES IS ROTATED COUNTERCLOCKWISE (LOOKING DOWN) FROM THE SECOND.

Pair	γ	θ
EGK, HFR	0.85	-9.8
EGK, EC4	0.70	-12.8
HFR, EC4	0.87	-5.7

Wind-current regression coefficients for the alongshelf components (R, Table V) show that the surface currents are more strongly coupled to the wind than those about two meters deeper. For the cross-shelf components the wind and currents are basically uncorrelated, which might be expected because the cross-shelf currents are primarily tidal. Both the principal axis analysis (Table IV) and the complex vector correlation (Table VI) provide estimates of the directional differences between the pairs. The magnitudes of the directional differences are small, i.e., 6º to 12º, and they are consistent in a counter-clockwise rotation (looking down) of currents with respect to wind, i.e., to the left of the wind. A clockwise rotation is expected at such shallow depths and has been reported by others, e.g. [4] The directional accuracy of the SeaSonde is rated at better than 7º, (ideal antenna patterns were used), while the accuracy of the 300-KHz Workhorse is 2º, and its calibration was checked before and after deployment. The Egmont Key wind station used here is not ideally situated for offshore wind observations of the study region. We attribute the counter-clockwise sense of rotation primarily to the location of the EGK coastal station, with possibly some contribution from direction measurement error in the current velocity observations.

CONCLUSIONS

Supplementing previous work [2], we compare wind, surface currents (0.5 m depth) measured by HF Radar and subsurface currents measured by the top bin (2.5 m depth) of a bottom-mounted ADCP on the WFS in 20-m water depth. The alongshelf surface currents measured by the radar are about 30% larger than those of the ADCP according to standard deviations and linear regression slopes. However, both instruments yield comparable tidal ellipse coefficients for the M_2 tide, which is barotropic and oriented approximately cross-shelf in the study area. Wind-current regression coefficients for the alongshelf show that the surface currents are more strongly coupled to the wind than those about two-meters deeper. For the cross-shelf components the wind and currents are basically uncorrelated, which might be expected because the cross-shelf currents are primarily tidal. Both the principal axis analyses and the complex vector correlations indicate directional differences of 6º to 12º in the near-surface layer, and they are consistent in a relative counter-clockwise sense of rotation (looking down) of currents with respect to wind, i.e., to the left of the wind. The location of the EGK coastal station, with possibly some contribution from direction measurement error in the current velocity observations probably accounts for the sense of rotation.

ACKNOWLEDGEMENT

The HF-Radar portion of this work was supported by the Texas General Land Office under the Interagency Cooperation Contracts 00-43R and 02-115R The USF investigators acknowledge support from the Office of Naval Research, Grant #N00014-98-1-0158 and the National Oceanic and Atmospheric Administration, Grant #NA76RG0463.

REFERENCES

[1] C. Teague, J. Vesecky, and D. Fernandez, "HF Radar instruments, past to present," *Oceanography*, vol. 10, no. 2, pp. 40-44, 1997.

[2] F. J. Kelly, R.H. Weisberg, J.S. Bonner, M.E. Luther, J.C. Perez, J.S. Adams, D Prouty, D. Trujillo, R. He, R. Cole, J. Donovan, and C.R. Merz, "An HF-Radar test deployment amidst an ADCP array on the West Florida Shelf," *Proceedings of the Oceans 2002 IEEE/MTS Conference*, October 29-31, 2002, Biloxi, MS, pp. 692-698, 2002.

[3] L. Shay, T. Cook, H. Peters, A. Mariano, R. Weisberg, P. An, A. Soloviev, and M. Luther, "Very high-frequency radar mapping of surface currents," *IEEE J. of Oceanic Eng.*, vol. 27, no. 2, pp. 155-169, April 2002

[4] C. C. Teague, J. F. Vesecky, and Z. R. Hallock, "A comparison of multifrequency HF Radar and ADCP measurements of near-surface currents during COPE-3," *IEEE J. of Oceanic Eng.*, vol 26, no. 3, July 2001.

[5] R. He and R. H. Weisberg, "Tides on the West Florida Shelf," *J. Phys. Oceanog.*, vol 32, no. 12, pp. 3455-3473, 2002.

[6] R. Weisberg, B. Black, and H. Yang, "Seasonal modulation of the West Florida continental shelf circulation," *Geophys. Res. Letters*, vol. 23, no. 17, pp. 2247-2250, August 1996.

[7] H. Yang, and R. Weisberg, " Response of the West Florida Shelf circulation to climatological wind stress forcing," *J. Geophys. Res.*, vol. 104, pp. 5301-5320, March 1999.

[8] M. G. G. Foreman, "Manual for Tidal Heights and Prediction," Pacific Marine Science Report 77-10, Inst. of Ocean Sciences, Patricia Bay, Sidney, B.C., 97 pp., 1977.

[9] W. Emery, and R. Thomson, *Data Analysis Methods in Physical Oceanography*. Pergamon, 634 pp., 1998.

[10] B. Reed, "Linear least-squares fits with errors in both coordinates. II: Comments on parameter variances," *Am. J. Phys*., vol. 60, no. 1, 1992.

[11] B. Reed, "Linear least-squares fits with errors in both coordinates," *Am. J. Phys*., vol. 57, no. 7, 1989.

[12] P. Sprent, and G. Dolby, "The geometric mean functional relationship," *Biometrics*, vol. 36, pp. 547-550, 1980.

[13] P. Kundu, "Ekman veering observed near the bottom," *J. Phys. Oceanogr.*, vol, 6, no. 2, pp. 238-242, 1976.

[14] R. Weisberg, B. Black, and Z. Li,, "An upwelling case study on Florida's west coast," *J. Geophys. Res.*, vol. 105, pp. 11459-11469, 2000.

DISCLAIMER